

Citation for the published version:

Merabet Boulouiha , H., Khodja, M., Rahiel, D., Allali, A., Kaddour, F., & Denai, M. (2018). Power Quality Enhancement in Electricity Grids with Wind Energy Using Multicell Converters and Energy Storage. Journal of Renewable and Sustainable Energy.

Document Version: Accepted Version © 2018 The Authors, reproduced by permission of 2018 AIP Publishing LLC.

General rights

Copyright© and Moral Rights for the publications made accessible on this site are retained by the individual authors and/or other copyright owners.

Please check the manuscript for details of any other licences that may have been applied and it is a condition of accessing publications that users recognise and abide by the legal requirements associated with these rights. You may not engage in further distribution of the material for any profitmaking activities or any commercial gain. You may freely distribute both the url (<http://uhra.herts.ac.uk/>) and the content of this paper for research or private study, educational, or not-for-profit purposes without prior permission or charge.

Take down policy

If you believe that this document breaches copyright please contact us providing details, any such items will be temporarily removed from the repository pending investigation.

Enquiries

Please contact University of Hertfordshire Research & Scholarly Communications for any enquiries at rsc@herts.ac.uk

Power Quality Enhancement in Electricity Grids with Wind Energy Using Multicell Converters and Energy Storage

^{1,3}H. Merabet Boulouiha, ²M. Khodja, ¹D. Rahiel, ³A. Allali, ³F. Kaddour, ⁴M. Denai

¹*Ecole Normale Polytechnique d'Oran ENPO, Algérie*

²*Centre universitaire de Relizane Ahmed Zabana CUR-AZ, Algérie*

³*Faculté de Génie Electrique, Département d'Electrotechnique*

LDDEE, Laboratoire de Développement Durable de l'Energie Electrique

Université des Sciences et de la Technologie d'Oran, Mohamed Boudiaf

⁴*School of Engineering & Technology, University of Hertfordshire, Hatfield AL10 9AB, UK*

houari.merabet@gmail.com, khodja1970@gmail.com, rahiel_djelloul@yahoo.fr, allalia@yahoo.com,

fouelectro@yahoo.fr, m.denai@herts.ac.uk

Abstract

In recent years, wind power industry is experiencing a rapid growth and more wind farms with larger size wind turbines are being connected to the power system. While this contributes to the overall security of electricity supply, large-scale deployment of wind energy into the grid also presents many technical challenges. Most of these challenges are one way or another, related to the variability and intermittent nature of wind and affect the power quality of the distribution grid. Power quality relates to factors that cause variations in the voltage level and frequency as well as distortion in voltage and current waveforms due to wind variability which produces both harmonics and inter-harmonics.

The main motivations behind serial switching cells are the ability to achieve high power with lower-size components and the improvement of waveforms at the input and output of the converter by increasing the number of degrees of freedom. This paper presents a new topology of static AC/DC/AC multicell converter to improve the power quality in grid-connected wind energy conversion systems. Furthermore, a battery energy storage system is included and a power management strategy is designed to ensure the continuity of power supply and consequently the autonomy of the proposed system. Simulation results are presented for a 149.2 kW wind turbine induction generator system and the results obtained demonstrate reduced harmonics, improved transient responses and reference tracking of the voltage in the wind energy conversion system.

Keywords: Wind energy, power quality, multicell converter, multicell neutral point clamped converter, indirect field-oriented control, induction generator, MPPT.

1. Introduction

Energy sustainability is a major challenge for the years ahead due to the rapidly increasing energy demand and global fossil fuel reserves going into decline within the next few decades. A larger adoption of alternative green energy based

on renewable resources is required to meet the ever-increasing global energy needs. Currently, wind and solar energies dominate the worldwide renewable electricity production. Wind energy installed capacity has taken such a proportion that grid operators are imposing new standards for the disconnection of decentralized electric power generation units. Disconnections following the triggering of wind farm protection equipment are no longer tolerated according to certain grid codes imposed by transmission and distribution system operators. To keep wind turbines connected to the grid even under certain grid fault conditions, new control schemes should be employed to improve the low voltage ride through (LVRT) capability of wind turbine generators [1-3].

In 1995, the International Electrotechnical Commission (IEC) launched a new standardization for the power quality of wind energy systems. In 1998, IEC published a draft of the IEC-61400-2 standard titled "Power Quality Requirements for Grid Connected Wind Turbines" [4].

The methodology of this IEC standard consists of three tests. The first is the analysis of flickers. IEC-61400-2 specifies a method that uses current and voltage time series measured at the terminals of wind turbine to simulate voltage fluctuations on the grid. The second relates to the switching operations of power electronics converter devices. This study was conducted for different wind speeds. The third test is related to harmonic analysis using fast-Fourier transform (FFT) techniques and the total harmonic distortion (THD) is calculated up to the 50th harmonic. In recent studies, high-frequency harmonics and inter-harmonics have been dealt with in IEC 61000-4-7 and IEC 61000-3-6 [5, 6]. In [7], it is stated that wind turbines produce not only harmonics but also inter-harmonics, i.e. harmonics that are not multiples of the network frequency (i.e. 50 or 60 Hz).

In recently published literature, multilevel converters have been proposed to improve the harmonic content of the output voltages that led to a reduction in the size or elimination of output filters [8-10]. Furthermore, the switching frequency of a multilevel converter can be reduced by 25 % to that of a conventional two-level converter, resulting in reduced switching losses [11,12].

Multicell series converters, introduced in the early 90s [13,14], consist of a serialization of elementary switching cells. This topology ensures equal stress distribution on the different low voltages semiconductor devices connected in series and improves the output waveforms and harmonic content when an adequate phase control strategy is applied. The multicell structure, however, requires the use of floating capacitors whose terminal voltages must be controlled and maintained at well-defined levels.

Different topologies of multi-level converters have been used in power systems applications and can be classified into the following five categories [15]: (i) Multilevel neutral-point clamped (NPC) configurations, (ii) Multi-level configurations with bidirectional switch, (iii) Multilevel configurations with floating capacitors, (iv) Multi-level configurations with several three-phase inverters, (v) Multi-level cascaded H-bridge configurations.

Recently, multicell converters topologies are being widely adopted to handle the continuously increasing power ratings of wind turbines and wind farms and address some of the related power quality issues.

AC side current ripples affect consumer's loads and can reduce the longevity or damage DC side components such as the capacitor or battery storage due to frequent discharging/charging [16-17]. Large current ripples in the capacitors can also cause a decline in the performance of inverters hence reducing their lifetime. The IEEE519 standard states

that the THD of AC currents should not exceed 5 %. Beyond this value, the lifetime all components of the microgrid is severely affected.

With the increasing penetration of distributed energy resources and smart grid technologies, the power grid is exposed to several other power quality issues including the continuity of supply, frequency fluctuations and voltage stability [18]. The rated voltage amplitude and frequency are considered as key indicators of quality of the power supply in a distribution network. In addition, energy supply to consumers should be without interruption. Voltage unbalance, harmonic level, increase in reactive power demand and frequency drops are the main energy quality issues affecting the distribution network. Energy quality problems in Smart Grids are studied in [19-23].

In [19-21], the authors proposed a PSO (Particle Swarm Optimization) based control strategy to improve the power quality in a stand-alone microgrid. This study focused on performance and quality parameters such as voltage regulation, frequency regulation as well as the THD of the current waveform. However, this control technique is not effective against harmonics generated from the switching of power converters.

In [22-24], the authors studied the performance of a microgrid with renewable energy sources connected with an Active Power Conditioner (APC). The work focused mainly on the improvement of harmonic current and power factor.

The authors in [22] proposed a control scheme based on Proportional-Integral (PI) regulators and a hysteresis Multilevel Inverter (MLI). The control strategy uses a compensation technique that forces the harmonic current in the microgrid to become balanced and sinusoidal. The main role of APC is to compensate harmonics, correct the power factor and balance the voltage. In [23], a photovoltaic system and a Shunt Active Power Filter (SAPF) connected to a nonlinear load is considered as a microgrid. The PAFP is controlled by a PWM hysteresis to improve the THD of the current in the microgrid connected to the distribution network. The main disadvantage of MLIs with hysteresis control is that the switching frequency variation generates large fluctuations of the current.

An active filter based on a three-level inverter has been studied in [24]. The filter is used to attenuate harmonics from a non-linear load and an unbalanced source. A fuzzy logic controller was used to improve the behavior of the voltage across the floating capacitor.

Multilevel converters can achieve high quality output voltages with a significant reduction of the THD, which leads to a reduction in the size of static converters and makes these topologies attractive for industrial applications [25-37]. A comparative study of three DTC (Direct Torque Control) methods for a squirrel cage induction generator (SCIG) was presented in [38]. Namely, the classical DTC, the DTC-SVPWM based on a fixed frequency two level and three-level Neutral Point Clamped (NPC) inverter topologies. The proposed three-level SVPWM topology takes into consideration the balancing the DC link voltage. These DTC techniques have also been compared with respect to their THD level. The modeling and control of a DFIG (Doubly-Fed Induction Generator) using a hybrid converter was proposed in [39]. The rotor side converter (RSC) consists of three identical two-cell converters implemented in parallel and the grid powers as well as the DC side voltage are controlled by a conventional converter.

A wind and solar photovoltaic hybrid system is proposed in [40, 41] where both renewable energy sources are connected to the DC link. The proposed hybrid power system is equipped with battery energy storage. In [41], the system is tested in abnormal network condition.

This paper focusses on developing a new AC/DC/AC converter topology and control scheme to improve the energy quality of a wind power system connected to the electricity network. Furthermore, a battery energy storage with a power management strategy is introduced to increase the efficiency and reliability of the distribution system.

The main objectives in this article are to analyse the quality of power in grid-connected wind energy conversion systems by adopting multicell power converter topologies to improve the THD level in the output voltage waveforms and integrating battery energy storage systems to ensure continuity of supply and enhance the autonomy and reliability of the proposed wind power system.

The remaining of the paper is organised as follows: Section 2 describes the wind energy conversion system which includes a flying capacitor multilevel AC/DC/AC converter topology (FCMC) driving a squirrel-cage induction generator (SCIG) connected to a smart load and a DC link connected to an energy storage system (ESS). Section 3 presents the control scheme of the SCIG and the MPPT strategy. The control design of the grid-side multicell converter is also developed in the Section 3. The power management and control of the battery energy storage is described in Section 4. The simulation results are presented in the Section 5. Finally, conclusions of the paper and future perspectives are discussed in Section 6.

2. Overview of the SCIG-based wind energy conversion system configuration

Fig. 1 depicts the wind energy conversion system (WECS) used in this work and its control scheme. The proposed circuit consists of a three-bladed wind turbine of radius R coupled to a variable-speed squirrel cage induction generator (SCIG).

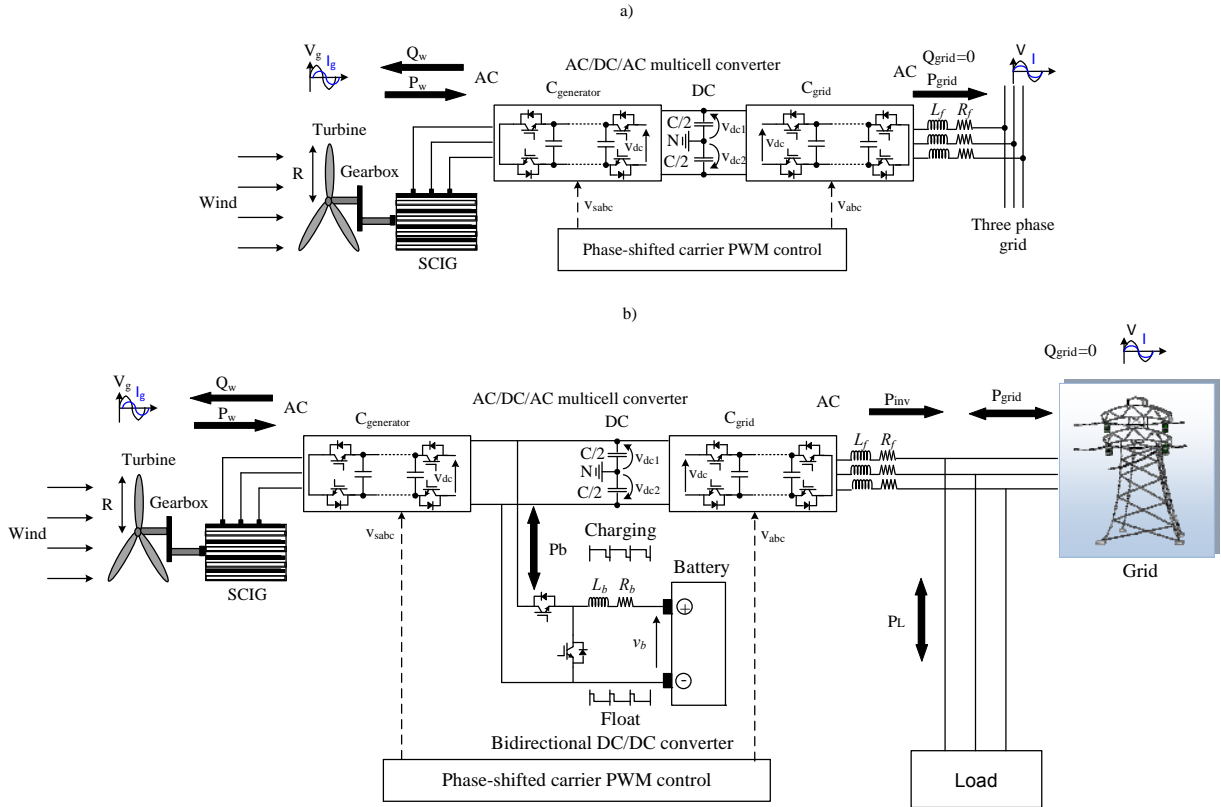


Fig. 1 SCIG-based WECS configuration. a) Basic circuit
b) Detailed circuit with energy storage.

The WECS is interfaced to the grid via two back-to-back multicell converters based on IGBTs (Insulated Gate Bipolar Transistor). One converter is connected to the stator of the generator while the other one is connected to the grid. This configuration allows a speed variation from 0 to 100 % of the nominal rotation speed.

The generator-side converter controls the converted power by adjusting the generator torque to achieve the desired rotational speed. The torque and the flux are controlled by the d-q components of the current of the generator in the rotating frame. The speed reference can be calculated from the wind speed to achieve optimal wind power extraction at low and medium wind speed ranges as well as at constant speed in high wind speed conditions when the power captured from the wind decreases.

The control of the grid-side inverter allows the control of power transfer from the WECS to the grid via the regulation of the DC voltage level.

The battery energy storage system is connected to the DC link via a bidirectional DC/DC converter to provide power flow in both directions (battery charge and discharge). The load consists of a neighborhood of homes equipped with PV panels and can exchange power with the power grid.

The power supply and demand equation is written as:

$$P_L = P_{grid} + P_b + P_w \quad (1)$$

Where P_{grid} , P_L , P_b and P_w denotes the powers of the grid, load, battery and wind generator respectively.

3. Multicell Converters Topologies and Control Schemes

3.1 Influence the number of the cells on the quality of the output voltages

The quality of the energy supplied to users depends on the voltage quality at the delivery point. Multicell AC/DC/AC converters have the ability to provide a better voltage output waveform with a reduced THD. Power quality may also be affected by external sources such as the failure of the power supply or other inherent installation faults.

The power circuit based on the multicell inverter has the following enhanced features [42]: (i) Increased voltage level: The addition of several switching cells in series makes it possible to reduce the voltage across the IGBTs and this leads to an increase in power transfer and an increase the operating voltage of the interconnected network, (ii) Increased bandwidth: By taking advantage of multicell-specific degrees of freedom, the inverter bandwidth can be easily improved as compared to other multi-level structures such as the Neutral Point Clamped (NPC) or the cascaded topology.

Fig.2 compares the THD of the voltage output from three, four and five levels multicellular converters for an amplitude modulation index M_i varied from 0.1 to 0.9. The results are obtained for a switching frequency of $f_{switch} = 3$ kHz.

The following can be noted:

- The lowest THD corresponds to the four-cell ($N = 4$) or five level inverter since it has the highest number of levels in the waveform of the converter output voltage.
- The largest THD corresponds to the two-cell ($N = 2$) or three-level inverter.

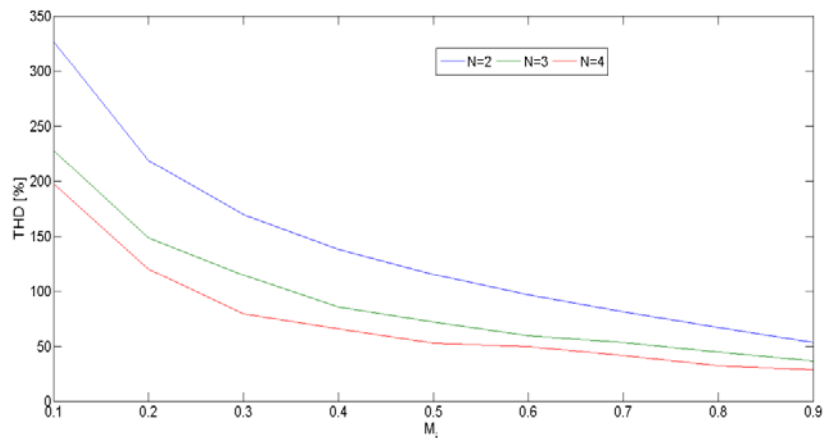


Fig. 2 Comparison of the THD of the multicell inverters for $N = 2, 3$ and 4.

The method of phase-shifted PWM is well detailed in [42].

3.2 Control of the generator-side converter

Recall that, indirect vector control or indirect field-oriented control (IFOC) is based on the estimation of the position of the flux vector. The voltages or currents required to maintain flux orientation and decoupling between the flux and torque are derived from the dynamic model of the machine. This method is easy to

implement and is more popular than the direct method, however, it is very sensitive to variations in the machine parameters.

IFOC strategy generates the desired control variables v_{sd}^* , v_{sq}^* and ω_r^* as a function of the two reference inputs (i_{sq}^* , ϕ_r^*) to achieve the decoupling between the flux and torque via the control of the direct (i_{sd}) and quadratic (i_{sq}) components of the stator current.

Fig. 3 describes the strategy of the IFOC based on rotor flux orientation for a variable-speed induction generator (IG).

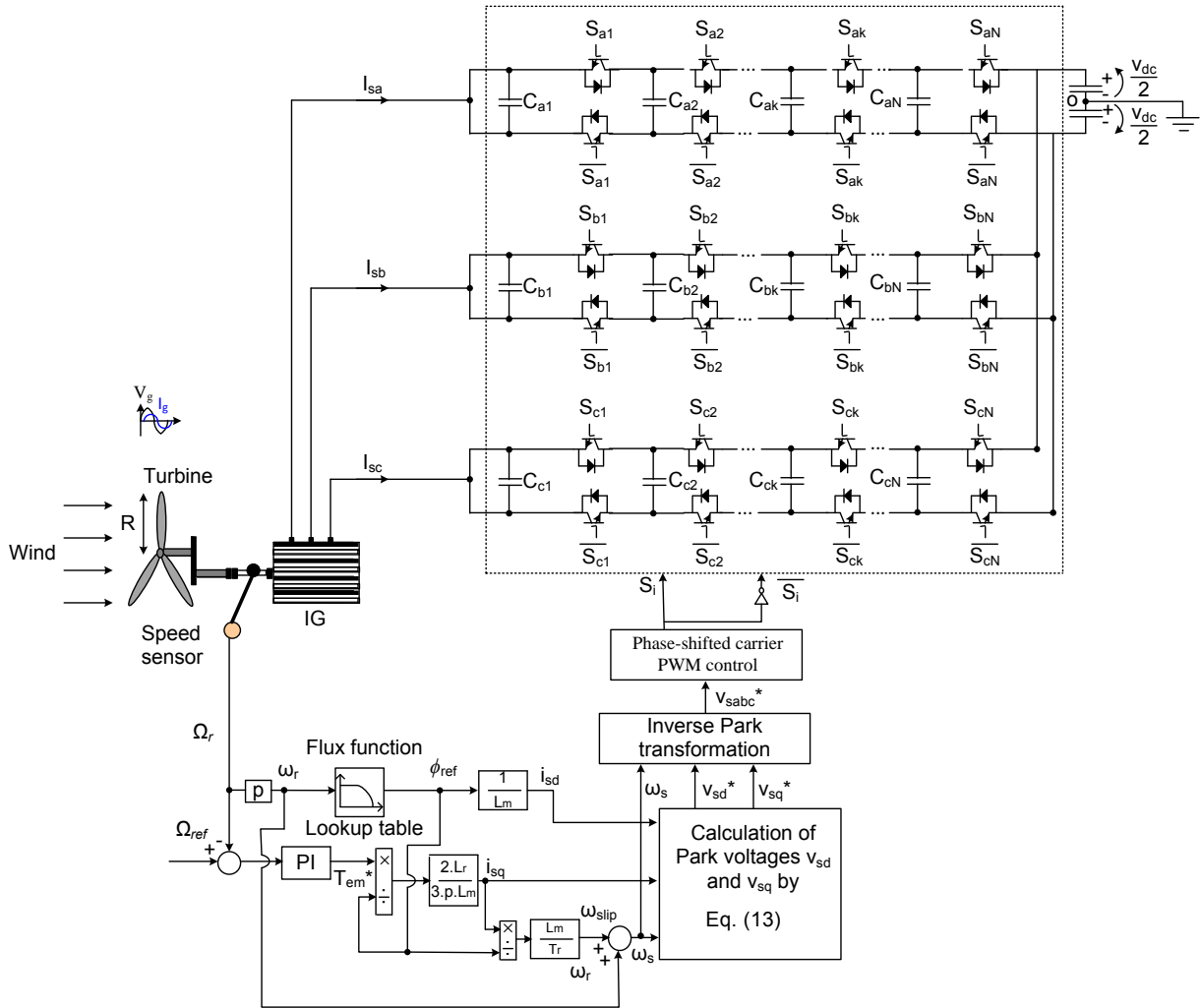


Fig. 3 IFOC scheme of the induction generator.

3.3 Control of the grid-side converter.

The role of the grid-side converter is to keep the DC bus voltage constant under any power flow conditions by generating the charging current required by the capacitor in particular during the start-up phase. The overall power system and its control scheme are depicted in Fig. 4.

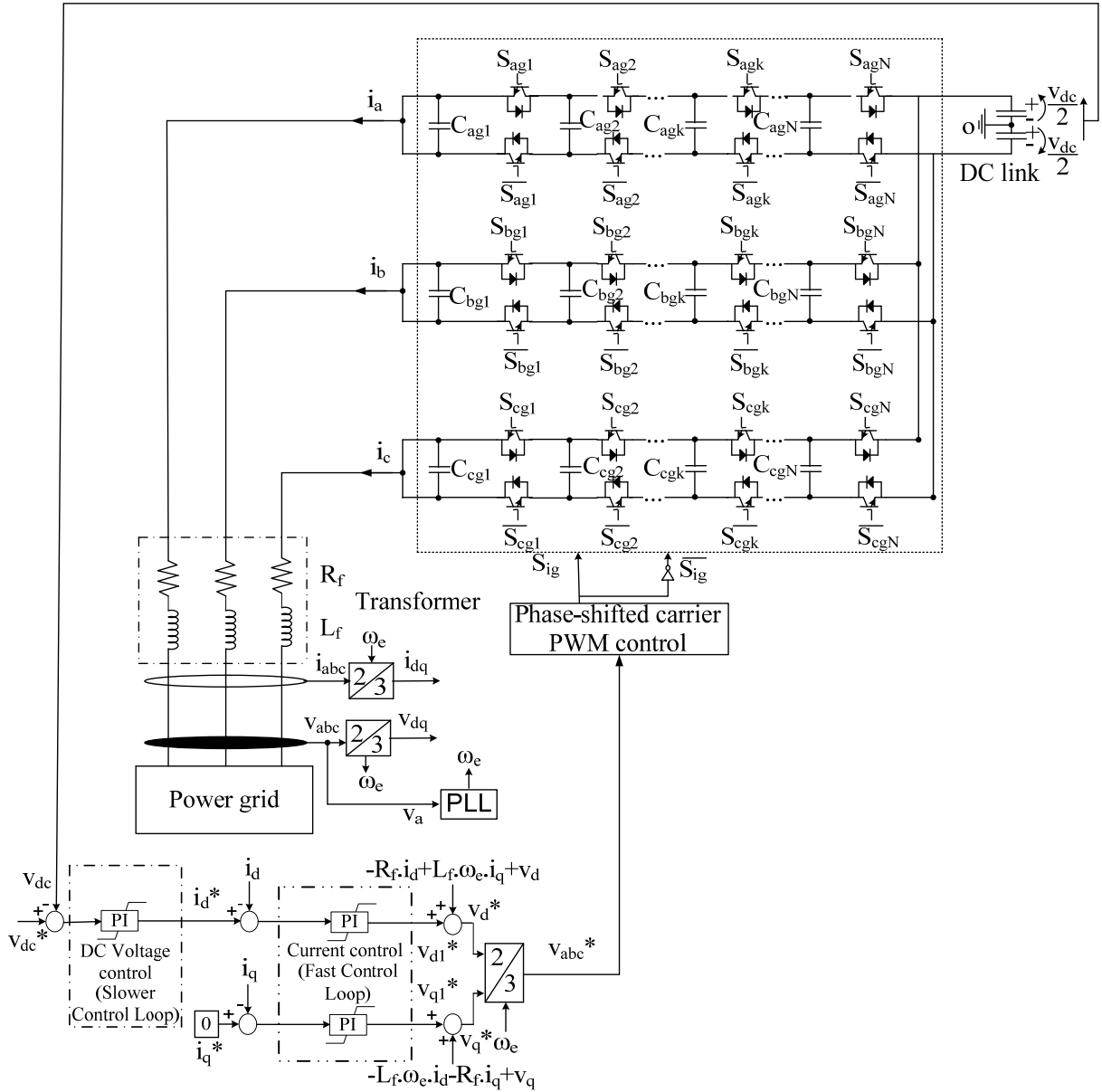


Fig. 4 Control scheme of the grid side multicell converter and DC bus.

4. Battery Power Management and Control

Energy storage improves the viability of renewable energy resources. From the network operator's perspective, distributed storage has the potential to reduce peak loads. During peak periods, each kilowatt-hour of energy consumed by local storage is one kilowatt-hour less supplied by the grid. It can also help increase the overall energy supply during peak periods and in the case of power grid outages, at a lower cost than other sources of generation.

Lithium-ion (Li-ion) is currently the most promising battery technology and among the best electrochemical batteries in the market. The cost is still significant compared to Lead batteries technology, but a decrease is expected in the coming years which would make Li-ion batteries the most viable technology for micro-grids [43].

This simulation study uses a storage unit consisting of a battery bank with a nominal voltage of 200 V connected directly to the DC bus. The battery bank model developed is based on the latest Li-ion technology, with high energy density, low self-discharge and maintenance-free which make it an ideal solution for residential applications. The main objective of using storage batteries in the DC bus is to support the grid system in cases of power network interruptions. Consequently, the battery will supply power to the load (discharging) or absorb power (charging) depending on the surplus of power available from the local generation.

The DC output of the generator side converter (PWM rectifier) of the wind turbine is connected to the DC bus which in turn is connected to the battery bank via a bidirectional DC-DC converter. The flowchart of Fig. 5 describes the proposed power management strategy for the battery to save energy and improve the lifetime of the storage device.

Two cascaded proportional integral (PI) controllers are used in the energy management system. The first controls the level of the battery voltage v_b and the second regulates the current according to the status of the powers. When the series chopper is controlled, the parallel chopper is idle, the battery consumes power ($i_b > 0$ the battery is charging), there is a transfer of electrical energy from the DC source v_{dc} to the battery. When the parallel chopper is controlled, the serial chopper is idle, the battery delivers a current to the load ($i_b < 0$ the battery is discharging).

In addition, a battery controller is used to maintain the state-of-charge (SOC) of the battery between 40-80 %.

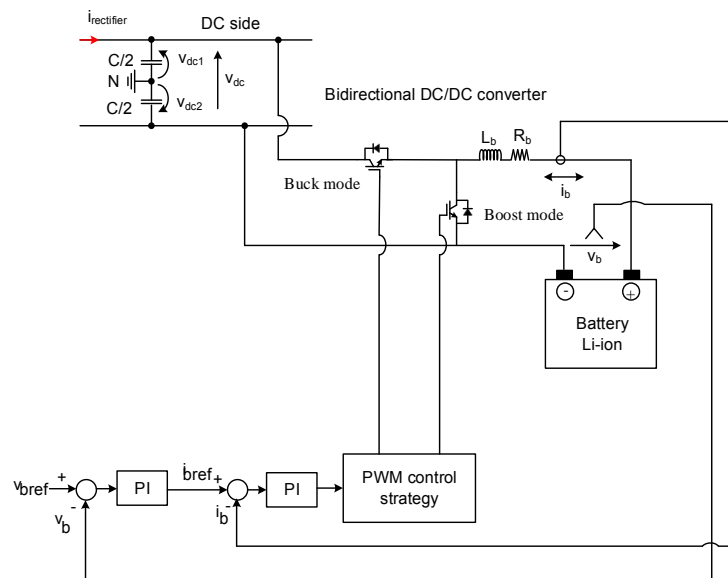


Fig. 5 Power management of the battery energy storage.

5. Simulations Results

The models for two, three, four and five level multicell AC/DC/AC converter topologies with IFOC strategy based on PSPMW modulation technique have been developed using Matlab/Simulink and SimPowerSystems toolbox.

The main motivation behind this simulation study was to investigate the benefits of using such multicell inverter topologies on the quality of energy delivered by the wind energy conversion system. The simulation scenarios considered are aimed to evaluate:

- ✓ the impact of using multicell topology on energy quality.
- ✓ the performance of the system when connected to smart load which consists of neighborhood of houses equipped with solar panels.

An analytic model is used to generate wind speed profiles to test the system under a wide range and more realistic operating conditions. The model used combines a white noise and a transfer function the parameters of which are a function of the characteristic values of the site and nature of the wind. The wind speed can be decomposed into two components: the rated turbulence component denoted $v_t(t)$ which models the wind speed. Over longer periods, the average wind characteristics in each site vary on a regular basis. This component is referred to as *slow component* and is denoted as $v_l(t)$.

Among the most popular methods to model the wind speed is the Van Der Hoven method [44]. In this model, the turbulence component is considered as a stationary random process and, therefore, does not depend on the variation of the average wind speed. The wind speed can be defined as follows:

$$v(t) = v_l(t) + v_t(t) = \frac{2}{\pi} \sum_{k=0}^{N_i} A_k \cos(\omega_k t + \varphi_k) + \frac{2}{\pi} \sum_{N_i}^N A_k \cos(\omega_k t + \varphi_k) \quad (2)$$

Where A_k represents the amplitude of each spectral component, ω_k is the pulsation in rad/s and φ_k denotes the phase in rad.

5.1 Power quality assessment for different multicell converter topologies

These simulations are aimed to assess the impact of different cell number on the power quality. The multicell inverter topologies investigated are two, three and four cells.

Fig. 6 represents the wind profile, the power coefficient C_p , the tip speed λ and the pitch angle β used in these simulations. It can be noted that for wind velocities less than 12 m/s, the pitch angle is zero and the power coefficient reaches its maximum value $C_p = C_{pmax}$ as well as the tip speed $\lambda = \lambda_{opt}$. Furthermore, for wind speeds greater than 12 m/sec, the power is equal to 149.2 kW which represents the nominal power of the generator. The pitch angle can be controlled by the orientation of the turbine blades to reject the extra power and ensure normal and safe operation of the generator.

Once the wind speed exceeds the nominal value of 12 m/sec, a decrease in power coefficient can be noticed. Under this constraint, the blades are controlled by adjusting the pitch angle as shown in Fig. 6 to reject the extra energy and keep the power at its nominal value of 149.2 kW.

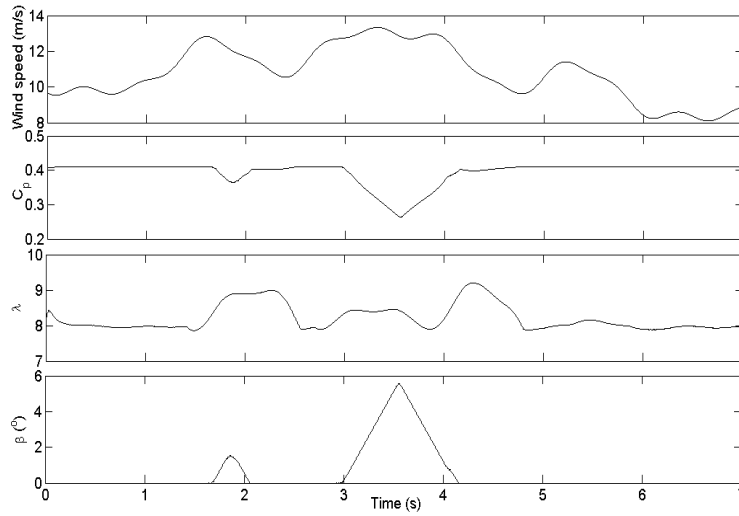


Fig. 6 Wind speed profile, power coefficient C_p , tip speed ratio λ and pitch angle β .

Fig. 7 shows the responses of the active and reactive powers of the DC/AC grid converter under the same wind profile of Fig. 6. From this figure, it can be observed that the waveforms of the real and reactive powers are smoother in the case of three- and four-cell multicell converters as compared to the two-cell converter.

The Fourier analysis is shown in Fig. 8 for the three multicell inverter topologies (two, three and four cells). It can be observed that the four-level topology leads to a quasi-sine wave current waveform and the THD is about 0.63 % whereas in the case of the two and three cells topologies the THDs are 1.47 % and 0.89 % respectively.

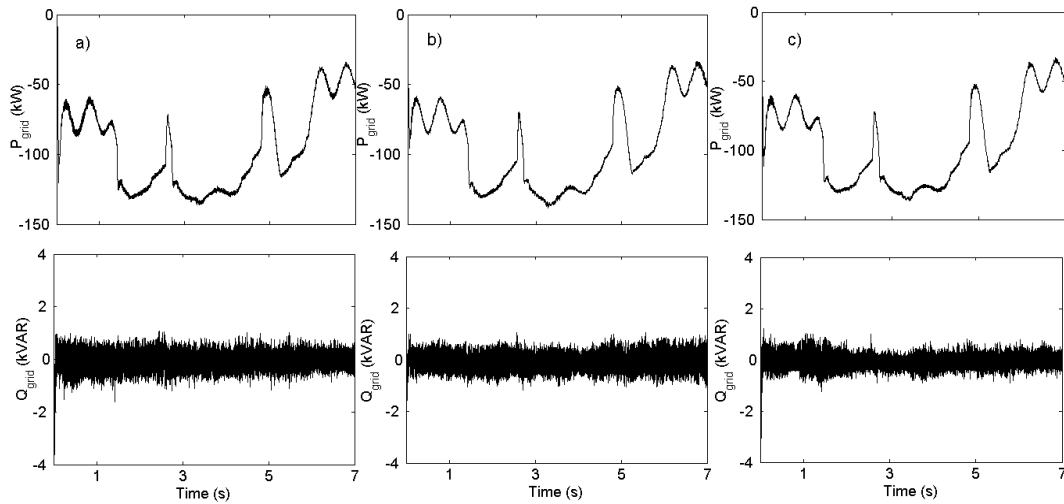


Fig. 7 Active and reactive power of the grid for a multicell inverter with:

(a) two cells, (b) three cells, (c) four cells.

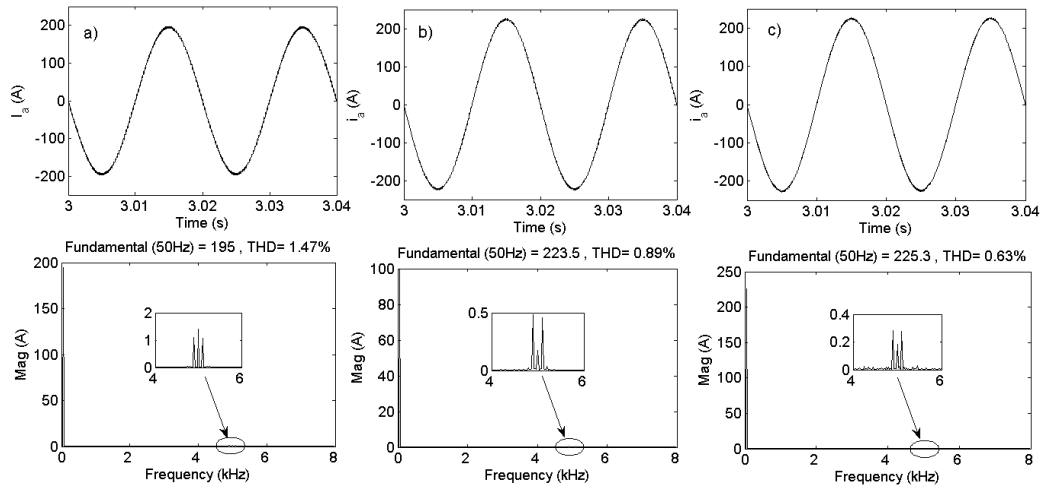


Fig. 8 Waveform of grid current of phase A and harmonic spectrum with the multicell inverter based on PSPWM. (a) two cells, (b) three cells, (c) four cells.

The following simulation results showing the waveforms of the rotor speed, electromagnetic torque, DC link voltage and powers are presented only for the two-cell converter topology. Similar responses are obtained for the other topologies.

Fig. 9 shows the rotor speed and the electromagnetic torque of the generator. It can be observed that for wind speeds less than 12 m/s, the torque and speed of the generator rotor vary with the wind speed profile of Fig. 6 and the rotor speed is the image of the electromagnetic torque. For wind speed greater than 12 m/s, the protection system is triggered to protect the wind turbine.

The generator is driven by a turbine with a mechanical torque T_m varying between -380 and -950 Nm. and produces an output power of -50 -149.2 kW to the network.

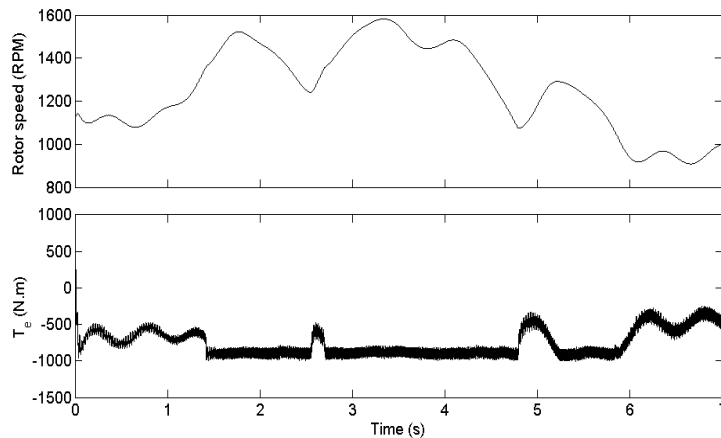


Fig. 9 Rotor speed and electromagnetic torque.

The DC bus voltage and the d - q components of the network current are shown in Fig. 10. Note that the DC link voltage v_{dc} follows its reference set at 1000 V. The real and reactive currents follow their references (for i_d the reference is set according to the available wind and for i_q the reference is set to zero).

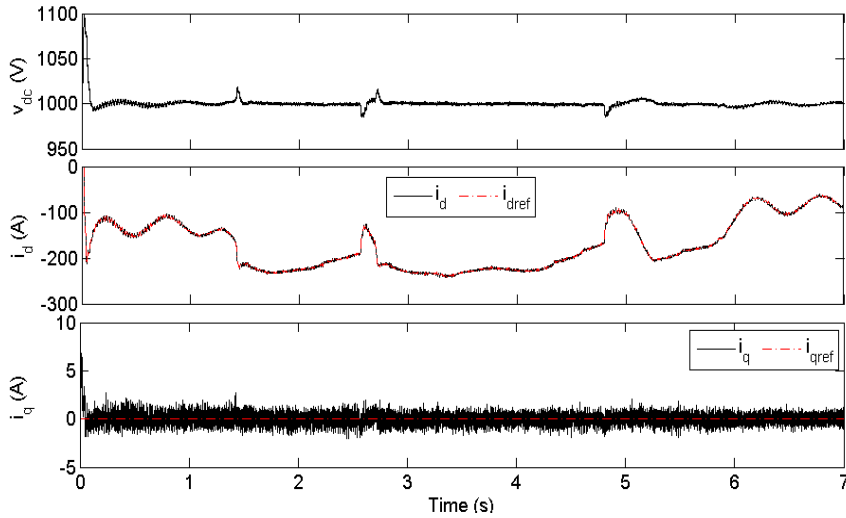


Fig. 10 DC link voltage, waveforms of the active and reactive currents.

Fig. 11 shows the real and reactive powers of the grid under the same wind profile of Fig. 6.

The variation of the wind speed between 8 and 13.5 m / s leads to a change of the point of maximum power which results in an adaptation of the modulation index to the new operating conditions as shown in Fig.11.

It can be observed that, for wind speeds exceeding 12 m/s, the wind power generated will not exceed its rated value even though the turbine is able to produce more power. This power limit is used to avoid possible rotor over-speed and protect the electrical system.

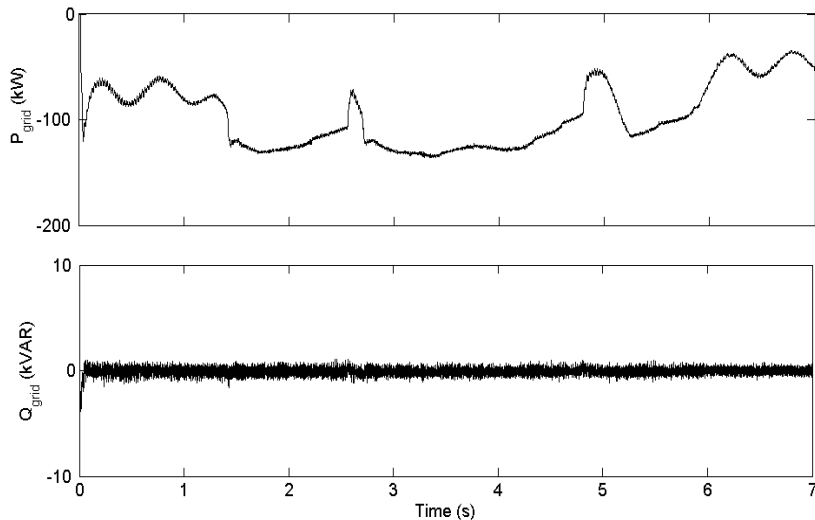


Fig. 11 Active and reactive power of the grid.

5.2 Variable load conditions

A. Variable load without storage system

In this section, the WECS is now connected to a neighborhood consisting of a group of houses equipped with solar panels as shown in Fig. 12.

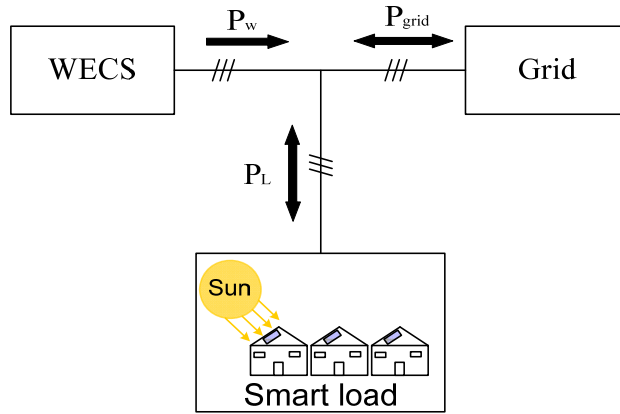


Fig. 12 WECS connected to the smart load.

With reference to Fig. 12, the power exchange between the grid, WECS and the load can be written as:

$$P_L = P_W + P_{grid} \quad (3)$$

Fig. 13 shows the real power profiles of each house. Each house can either consume or generate power which leads to a bidirectional energy exchange with the grid.

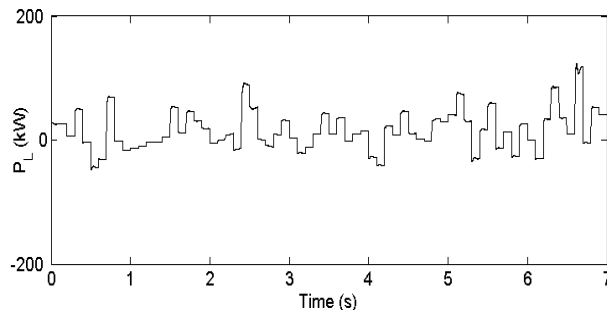


Fig. 13 Real power of the load.

The real and reactive powers of the grid are illustrated in Fig. 14 where it can be observed that the four-cell multicell inverter leads to the smoothest waveform. Depending on the load power requirement, the real power of the grid can be positive (when power is being injected into the grid), zero (when no power is supplied from the grid i.e. the WECS is able to satisfy the load demand) and negative (when the load power requirement exceeds the available power from the WECS). The reactive power of the grid is smoother in the case of a four-cell inverter as compared to the two and three-cell inverters. This demonstrates the advantage of using a four-cell converter topology.

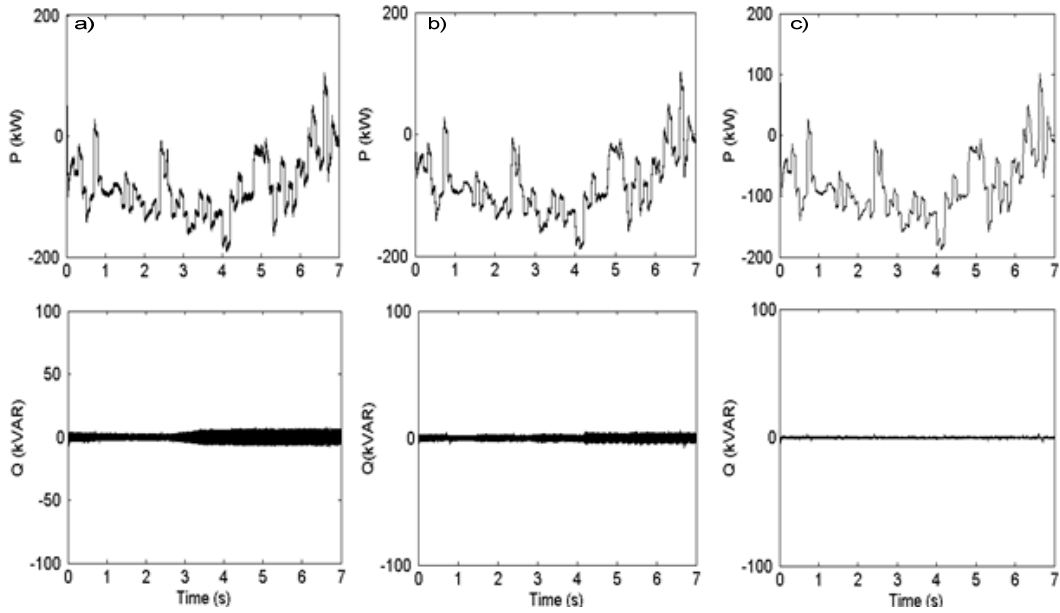


Fig. 14 Real and reactive power of the grid for the multicell inverter.

(a) two cells, (b) three cells, (c) four cells.

Fig. 15 shows the responses of real and reactive power of the grid-side inverter with three, four and five levels respectively. A significant improvement can be observed with the five-level converter.

It may be noted that the spikes due the opening and closing of power electronic switches. Have been significantly attenuated in the case of the five-level converter as compared to the other two converter topologies.

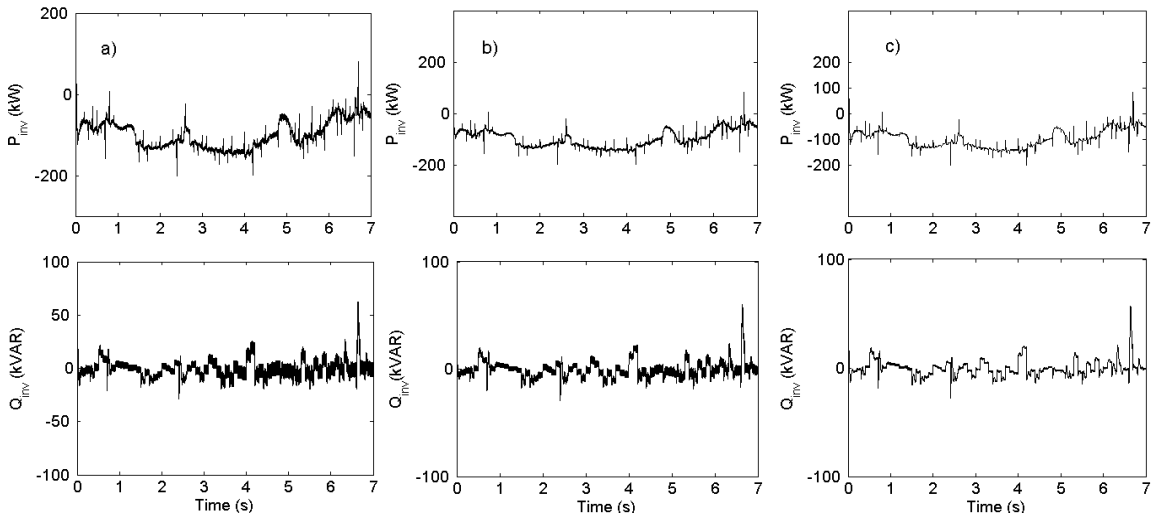


Fig. 15 Real and reactive power of the inverter for the multicell inverter.

(a) three levels, (b) four levels, (c) five levels.

B. Variable load with storage system

The wind power system can operate up to a maximum output of 149.2 kW, corresponding to a maximum wind speed of 12 m/s, therefore a battery energy storage system (BESS), which would serve as a buffer for balancing generation and demand, would be beneficial. A battery energy storage system (EES) is now introduced as shown in the Fig. 16.

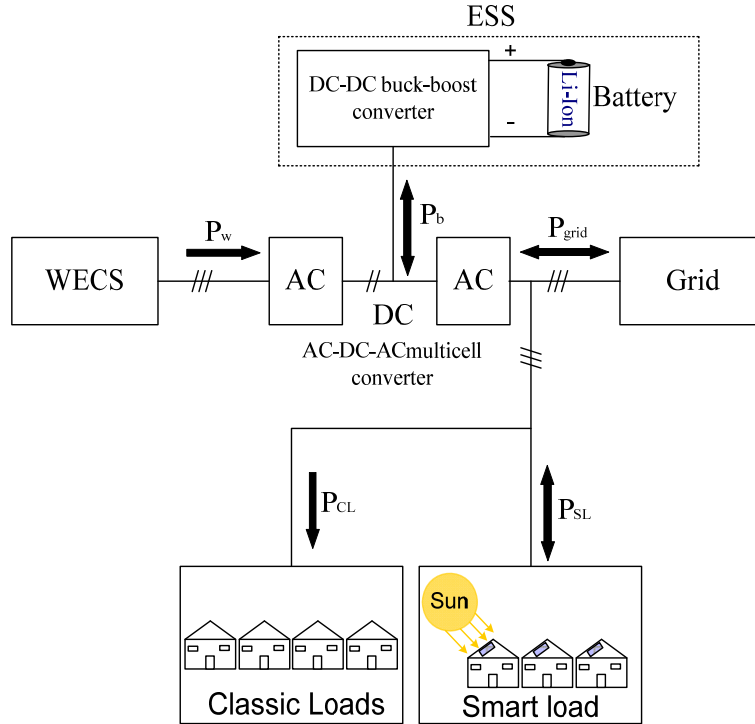


Fig. 16 Integration of the battery energy storage system.

The load power becomes:

$$P_L = P_{SL} + P_{CL} \quad (4)$$

The random profile of the wind speed is shown in Fig. 17. It can be noticed that the wind speed is in the range 4-18 m/s. The fluctuating component of the wind speed is modeled as a stationary Gaussian random process.

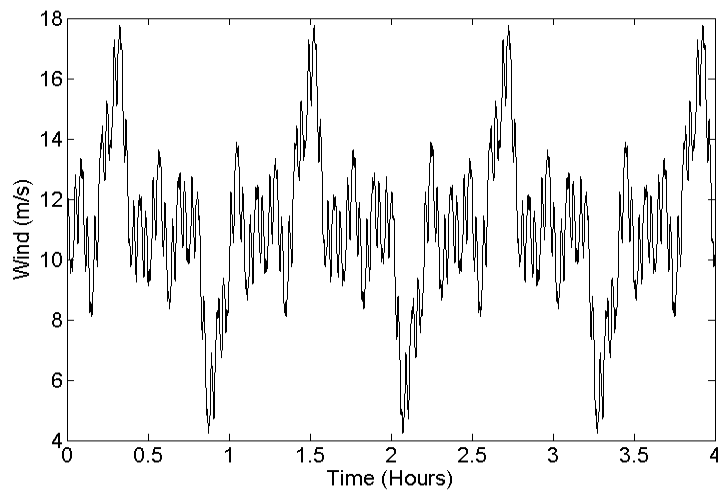


Fig. 17 Wind speed profile.

Fig. 18 represents the powers of the load (smart load and classic load) and smart load which varies between -30 kW (generation) and +60 kW (consumption).

The sign of the smart load power defines the direction of power consumption. The total power P_L is the sum of the conventional P_{CL} power and the power P_{SL} of the smart load. The latter is positive, which indicates that the load is always consuming active power.

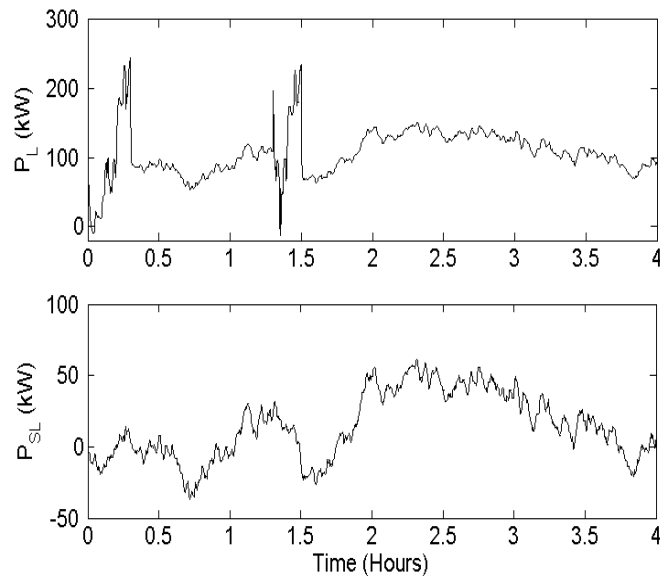


Fig. 18 Powers of load and smart load.

Fig. 19 shows the power of grid which varies between +200 kW and -200 kW.

Network outages have been simulated to test the operation of the overall system under. The periods of the power cuts are chosen in the range [7.2-18 minutes] and [1 hour and 18 min-1 hour 30 min] which respectively gives mains cutoff times of 10.2 and 12 minutes. In these periods the power grid is zero. Outside this period, the power of the grid is varied according to the following situations: (i) if the power is positive and the grid provides power to the load. (ii) if the sign of the power is negative, the grid is consuming the extra power.

An imbalance between production and consumption induces a change in the frequency due to the wind turbine and generator speed variation. This variation can cause fluctuations in the voltage. To overcome these problems, an energy storage system was installed in the DC side as shown in Fig. 16. The main role of this storage system is to provide power during emergencies such as power outages as shown in Figs. 19 and 20. This reduces the fluctuations in the voltages and increase the degree of stability and thus improving therefore the quality of energy. In the case of a failure or disconnection of the main supply as shown in Fig. 19, the extra energy is stored in the batteries (if the power generated is greater than that required by the load). If the production is lower than the consumption, the battery system the power required by the load.

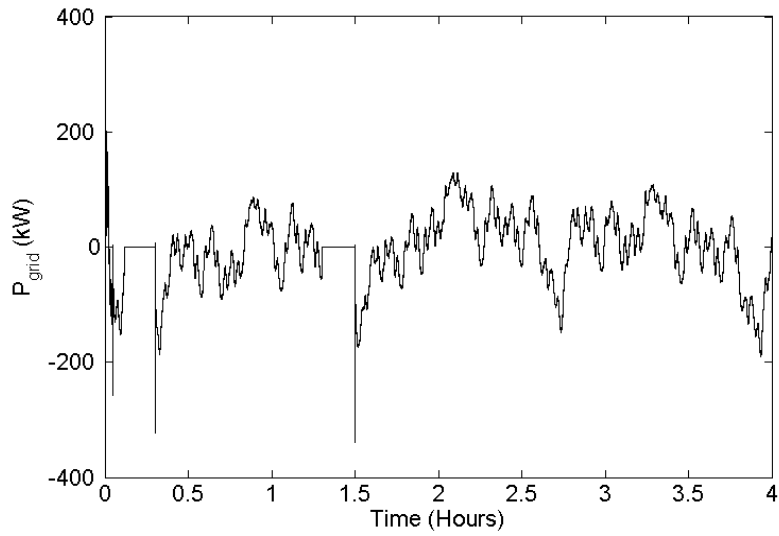


Fig. 19 Power of the grid.

Fig. 20 shows the power and current of the BESS. The BESS is operated in the case where the network cannot support the local generation (wind and PV in smart load). From Fig. 20, it can be noted that the BESS system consumes additional power which charges the storage batteries. However, in the case when generation is less than consumption, the BESS system provides the extra power required by the load (intelligent management of stored power).

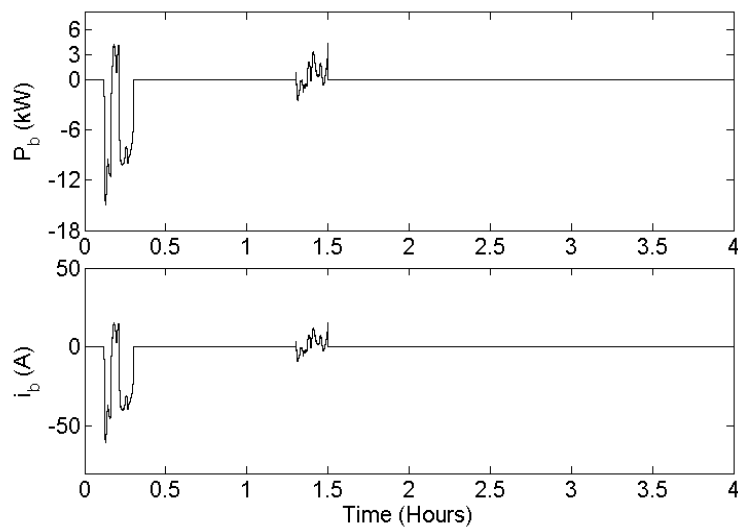


Fig. 20 Power and current of the battery.

Fig. 21 shows the SOC of BESS. Initially, the battery is charged at 80 % (upper limit). When the powers generated by wind and PV of smart grid systems cannot satisfy the load, the battery will supply the required power to the load. In the case where the wind power is sufficient to satisfy the load demand, then the battery, if not sufficiently charged, will be charged from the surplus of power from the wind, if any, or directly from the grid.

It can be noted that there are two modes of operation of the BESS:

- ✓ Idle state: in this case, there is no energy exchange between the battery and the system. The SOC is constant during this period.
- ✓ Active state: this is the operating state where the battery can generate or consume active power.

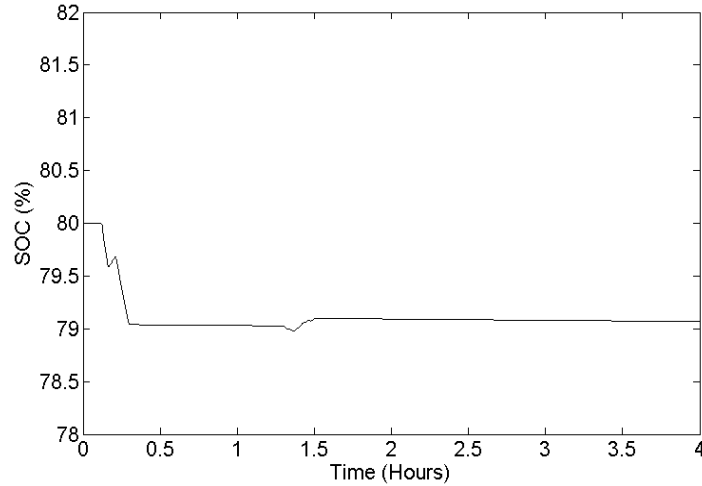


Fig. 21 State of charge for the battery.

Fig. 22 shows the response of the DC bus voltage which is successfully controlled at its reference of 1000 V. The charge and discharge of the battery appear as spikes in the DC voltage waveform.

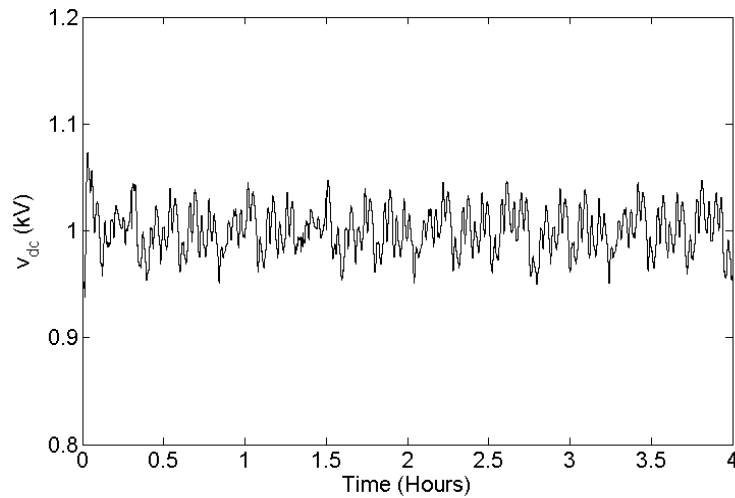


Fig. 22 DC link voltage.

6. Conclusion

Advanced power electronics, information and communication infrastructures, advanced control and advanced demand response strategies are key enabling technologies that will help optimize the operation of the electrical power system. In this article, a thorough simulation study was presented to assess the impact of using advanced power electronics and storage systems on the quality and stability of typical grid-integrated smart energy system consisting of local generation

and energy storage. This simulation study was, primarily, aimed at investigating various multicell converter topologies and their contribution to the improvement of energy quality of the overall system.

The paper proposed a topology of AC/DC/AC multicell converter based on the series-connected switching cells for wind turbine applications. There are several advantages of the multicellular converter structure over the conventional two-level. Among these, a reduction in the harmonic content and hence an improvement of the output waveform of the voltage and a reduction of the voltage stress on the switches (this is proportional to the number of levels). The series topology is also more flexible (relative to the NPC structure) since different voltage levels can be easily obtained and allows natural balancing of floating voltages.

On the other hand, the main disadvantages of this structure are that it requires many capacitors especially for a three-phase configuration. It should also be noted that the capacitors operating voltages are different depending on the position in the "multi-level cell" (cost, weight, assembly, etc.) and the converter control technique to balance the voltage of each capacitor can be quite challenging. However, for a three-phase configuration, the control of each arm to achieve the balancing of the capacitors' voltages can be performed independently which reduces the complexity of the control scheme and makes it more flexible.

Power quality is achieved by maintaining the characteristic parameters of voltage and current waveforms of the electric network and the continuity and reliability of supply of power to customers.

This work is mainly focused on the power quality issues when wind turbines are connected to the grid and how these can be mitigated using multi-cell converter topologies combined with an energy storage system. The power quality aspects addressed in this study are the improvement of the voltage waveforms by a reduction of the harmonic content, and continuous and reliable energy supply to the load. Due to the intermittency of WECS, a power management strategy is proposed for the energy storage system to ensure that the load is supplied without interruption.

It is worth mentioning that the harmonics due to the opening and closing of the switches of AC/DC/AC converters can increase the ripple voltage on the DC side. The effect of these ripples can reduce the lifetime of the batteries connected at the DC side of the wind energy conversion system. In addition, these ripples cannot only affect the operation of the batteries but also the DC side capacitor. Fourier spectral analysis has shown that harmonics of order $N \times f_{switch}/f_m$ are shifted towards high frequencies which improves the quality of the three-phase currents and makes the filtering of these harmonics easier. The five-level multicell topology generates high frequency harmonics which can be shifted further away from the fundamental frequency. This leads to a better quality of the currents waveforms at the output of the AC/DC/AC converter.

Several simulation scenarios were performed under MATLAB/Simulink to evaluate the performance of different converter topologies. The results showed an enhanced performance of WECS with a substantial reduction in THD in the output current of the AC/DC/AC converter. The THD of the grid currents has been reduced to 0.63 % with the five-level multicell inverter as compared to the three- and four-level topologies where the THD was 1.47 % and 0.89 % respectively with a 5 kHz switching frequency.

7. References

- [1] Qi L., Langston J., Steurer M., “Applying a STATCOM for Stability Improvement to an Existing Wind Farm with Fixed-Speed Induction Generators”, Power and Energy Society General Meeting – Conversion and Delivery of Electrical Energy in the 21st Century, 2008 IEEE, page(s): 1-6, 20-24 July 2008.
- [2] Muljadi E., Butterfield C. P., Conto J., Donohoo K., “Ride-Through Capability Predictions for Wind Power Plants in the ERCOT Network”, Power Engineering Society General Meeting, 2005. IEEE, page(s): 72- 79 VoU, 2-16 June 2005.
- [3] Fadaeinedjad R., Moschopoulos G., “Using STATCOM to Mitigate Voltage Fluctuations Due to Aerodynamic Aspects of Wind Turbines”, IEEE Power Electronics Specialists Conference, PESC 2008, 15-19 June 2008 pp:3648 3654.
- [4] Foussekis D., Kokkalidis F., Tentzevakis S., and Agoris D., “Power quality measurement on different type of wind turbines operating in the same wind farm”, presented at EWEC 2003.
- [5] International Electrotechnical Commission, IEC Standard, Amendment1 to Publication 61000-4-7, Electromagnetic Compatibility, General Guide on Harmonics and Inter-harmonics Measurements and Instrumentation, 1997.
- [6] International Electrotechnical Commission, IEC Standard, Publication 61000-3-6, Electromagnetic Compatibility, Assessment of Emission Limits for Distorting Loads in MV and HV Power Systems, 1996.
- [7] Ake L., Poul S. and Fritz S., “Grid impact of variable speed wind turbines”, presented at EWEC’ 99.
- [8] Tolbert L. M., Peng F. Z., and Habetler T. G., “Multilevel converters for Large Electric drives” IEEE Transactions on Industry Applications, Volume 35, Issue 1, Page(s):36 – 44.
- [9] Rodriguez J., Lai J.S., and Peng F. Z., “Multilevel inverters: a survey of topologies, controls, and applications”, IEEE Transactions on Industrial Electronics, Volume 49, Issue 4, Aug. 2002 Page(s):724 – 738.
- [10] Céspedes M., Sun J., “Modeling and mitigation of harmonic resonance between wind turbines and the grid”, in Energy Conversion Congress and Exposition (ECCE), 2011 IEEE, pp. 2109{2116, IEEE, 2011.
- [11] Marchesoni M., Mazzucchelli M., “Multilevel converters for high power AC drives: a review”, in Proc. IEEE International Symposium on Industrial Electronics, ISIE’93 - Budapest, Page(s):38 – 43, 1993.
- [12] Wang J., Burgos R., Boroyevich D., “A survey on the modular multilevel converters #x2014; modeling, modulation and controls”, in Energy Conversion Congress and Exposition (ECCE), 2013 IEEE, pp. 3984{3991, Sept 2013.
- [13] Meynard T. A., Foch H., “Multi-level choppers for high voltage applications”, *Journal of European Power Electronics and Drives*, vol. 2, no. 1, pp. 45–50, March 1992.
- [14] Meynard T. A., Foch H., Forest F., Turpin C., and all, “ Multicell converters: Derived topologies”, IEEE Trans Ind. Electron 49(5):978–987 (Special Issue on Multilevel converters, October 2002)
- [15] Bum-Seok S., Sinha G., Manjrekar M. D., Lipo T. A., “Multilevel Power Conversion – An Overview of Topologies and Modulations Strategies”, in Proceedings of the International Conference on Optimization of Electrical and Electronic Equipments, 1998. OPTIM '98. Volume 2, Page(s):AD-11 - AD-2.

- [16] Ma T., Yang H., Lu L., "A feasibility study of a stand-alone hybrid solar–wind–battery system for a remote island", *Applied Energy* 121 (2014) 149–158.
- [17] Zhu X., Xia M., Chiang H. D., "Coordinated sectional droop charging control for EV aggregator enhancing frequency stability of microgrid with high penetration of renewable energy sources", *Applied Energy* (2017)
- [18] Meradi S., Benmansour K., Herizi K., Tadjine M., Boucherit M.S., "Sliding mode and fault tolerant control for multicell converter four quadrants", *Electric Power Systems Research* 95 (2013) 128–139.
- [19] Al-Saedi W., Lachowicz S. W., Habib D., Bass O., "Power quality enhancement in autonomous operation using Particle Swarm Optimization", *International Journal of Electrical Power & Energy System*, vol. 42, no. 1, pp. 139–149, 2012.
- [20] Al-Saedi W., Lachowicz S. W., Habib D., Bass O., "Power flow in grid connected microgrid operation using Particle Swarm Optimization under variable load conditions", *International Journal of Electrical Power & Energy System*, vol. 53, no. 1, pp. 742-751, 2013.
- [21] Al-Saedi W., Lachowicz S. W., Habib D., Bass O., "Voltage and frequency regulation based DG unit in an autonomous microgrid operation using Particle Swarm Optimization", *International Journal of Electrical Power & Energy System*, vol. 53, no. 1, pp. 742-751, 2013.
- [22] Vechiu I., Gurguiatu G., Rosu E., "Advanced active power conditioner to improve power quality in microgrids", in *Proceedings of the 9th International Power and Energy Conference (IPEC)*, pp. 728-733, Singapore, October 2010.
- [23] Mishra C. S., Jena R. K., Mishra G. S., "Power Quality Enhancement of Micro-Grid Using DG and Power Quality Conditioner", *Second international Conference on Electrical, Computer and Communication Technologies (ICECCT)*, IEEE, February 2017.
- [24] Saidi S., abbassi R., Chebbi S. "Fuzzy logic controller for three-level shunt active filter compensating harmonics and reactive power", *International Journal of Adaptive Control and Signal Processing* 30 (6), 809-823, 2016.
- [25] Ashraf Gandomi A., Varesi K., Hosseini S. H., "Control strategy applied on double flying capacitor multi-cell inverter for increasing number of generated voltage levels", *IET Power Electron.*, 2015, Vol. 8, Iss. 6, pp. 887–897.
- [26] Babaei E., Alilu S., Laali S., "A new general topology for cascaded multilevel inverters with reduced number of components based on developed H-bridge", *IEEE Transactions on Industrial Electronics.*, 2014, 61, (8); pp. 3932–3939.
- [27] Gupta K.K., Jain S., "A novel multilevel inverter based on switched DC sources", *IEEE Transactions on Industrial Electronics*, 2014, 61, (7); pp. 3269–3278.
- [28] A.K. Sadigh, S.H. Hosseini, M. Sabahi, G.B. Gharehpetian, "Double flying capacitor multicell converter based on modified phase-shifted pulse width modulation", *IEEE Transactions on Power Electronics*, 2010, 25, (6); pp. 1517–1526.
- [29] Dargahi V., Abarzadeh M, A. Sadigh K., Dargahi S., "Elimination of DC voltage sources and reduction of power switches voltage stress in stacked multicell converters: analysis, modeling, and implementation", *Int. Trans. Electr. Energy Syst.*, 2014, 24, (5), pp. 653–676.

- [30] Dargahi V., Sadigh A.K., Abarzadeh M., Pahlavani M.R.A, Shoulaie A., “flying capacitors reduction in an improved double flying capacitor multicell converter controlled by a modified modulation method”, *IEEE Trans. Power Electron.*, 2012, 27, (9), pp. 3875–3887.
- [31] Sadigh A.K., Dargahi V., Abarzadeh M., Dargahi S., “Reduced DC voltage source flying capacitor multicell multilevel inverter: analysis and implementation”, *IET Power Electron.*, 2014, 7, (2), pp. 439–450.
- [32] Ajami A., Oskuee M.R.J., Mokhberdoran A., Van den Bossche A., “Developed cascaded multilevel inverter topology to minimise the number of circuit devices and voltage stresses of switches”, *IET Power Electron.*, 2014, 7, pp. 459–466.
- [33] Kai-Ming T., Wai-Lok C., “Multi-level multi-output single-phase active rectifier using cascaded H-bridge converter”, *IET Power Electron.*, 2014, 7, pp. 784–794.
- [34] Ajami A., Shokri H., Mokhberdoran A., “Parallel switch-based chopper circuit for DC capacitor voltage balancing in diode-clamped multilevel inverter”, *IET Power Electron.*, 2014, 7, pp. 503–514.
- [35] Marchesoni M., Tenca P., “Diode-clamped multilevel converters: a practicable way to balance DC-link voltages”, *IEEE Trans. Ind. Electron.*, 2002, 49, pp. 752–765.
- [36] Adam G.P., Williams B.W., “New emerging voltage source converter for high-voltage application: hybrid multilevel converter with dc side H-bridge chain links”, *IET. Gener. Transm. Distrib.* 2014, 8, pp. 765–773.
- [37] Zha X., Xiong L., Gong J., Liu F., “Cascaded multilevel converter for medium-voltage motor drive capable of regenerating with part of cells”, *IET Power Electron.*, 2014, 7, pp. 1313–1320.
- [38] Merabet Boulouiha H., Allali A., Laouer M., Tahri A., Denai M., Draou A., “Direct torque control of multilevel SVPWM inverter in variable speed SCIG-based wind energy conversion system”, *Renewable Energy* 80 (2015) 140–152.
- [39] Taibi F., Tadjine M., Seghir Boucherit M., Benzineb O., “Hybrid Control of DFIG Using Multicell Converters. Control”, *Engineering & Information Technology (CEIT)*, 2015 3rd International Conference on, Pages: 1-6, IEEE 2015.
- [40] Abbassi R., Chebbi S. "Energy Management Strategy for a Grid-Connected Wind-Solar Hybrid System with Battery Storage: Policy for Optimizing Conventional Energy Generation. *International Review of Electrical Engineering (I.R.E.E.)*; 7: 3979-90.
- [41] Abbassi R., Saidi S., Hammami M. and Chebbi S. "Analysis of Renewable Energy Power Systems: Reliability and Flexibility during Unbalanced Network Fault", *Handbook of Research on Advanced Intelligent Control Engineering and Automation*, Volume 1, Issue 24, pp. 651-686.
- [42] Khodja M., Rahiel D., Benabdallah M.B., Merabet Boulouiha H., Allali A., Chaker A., Denai M., "High Performance Multicell Series Inverter-Fed Induction Motor Drive", *Electrical Engineering*, Springer, Vol.98, No4, December 2016.
- [43] ESA. (2007). Technologies and comparisons.
- [44] Roy Sambatra E.J., “Simulation d’une chaîne de conversion d’énergie éolienne à base d’une génératrice synchrone à aimants permanents pour un site isolé”, *JCGE’03*, Saint-Nazaire, 5 et 6 juin 2003.

- [45] Uchechi O., Peter J., Linda W., Angele R., “Comparison of two residential Smart Grid pilots in the Netherlands and in the USA, focusing on energy performance and user experiences”, Elsevier, Applied Energy 191 (2017) 264–275.
- [46] Melicio R, Mendes VMF, Catalao JPS, “Transient analysis of variable-speed wind turbines at wind speed disturbances and a pitch control malfunction”, Elsevier J Appl Energy (2011) 88:1322–1330.
- [47] Dicorato M, Forte G, Trovato M, ‘Wind farm stability analysis in the presence of variable-speed generators’. Elsevier J Energy (2012) 39:40–47.
- [48] Vepa R., “Nonlinear, optimal control of a wind turbine generator”, IEEE Trans Energy Convers (2011).
- [49] Abedini A, Nikkhajoei H., “Dynamic model and control of a wind-turbine generator with energy storage”. IET Renew Power Gener (2011).
- [50] Dargahi V., Sadigh A. K., Abarzadeh M., Alizadeh M. R., Shoulaie A., “Power Electronics in Small Scale Wind Turbine Systems”, Power Elec- tronics, IEEE Transactions on. (2012), 27(9), 3875-3887.
- [51] Abarzadeh, M., “Modelling Design Implementation of Grid Connected Small Scale Wind Generation & System”, Msc thesis. Sahand University of Tech; (2011).

APPENDIX A

Table 1: **Parameters of the Simulation Models**

Grid	
Effective voltage, V_s [V]	460
Frequency, f_s [Hz]	50

Transformer	
Leakage resistance, R_f [Ω]	0.2
The leakage inductance, L_f [mH]	2

Turbine	
Density area, ρ [kg.m ⁻²]	1.225
Nominal mechanical power, $P_{m,n}$ [kW]	149.2
Radius of the turbine, R [m]	10.5
Nominal wind speed, v_n [m.s ⁻¹]	12
Gain of the multiplier, G	17.1806

SCIG	
Nominal power, P [kW]	149.2
Nominal frequency, $f_{g,n}$ [Hz]	50

Stator resistance, R_s [m Ω]	14.85
Stator leakage inductance, L_{ls} [mH]	0.3027
Rotor resistance, R_r [m Ω]	9.295
Rotor leakage inductance, L_{lr} [mH]	0.3027
Cyclic mutual inductance, L_m [mH]	10.46
Inertia, J [kg.m ²]	3.1
Viscous friction coefficient, f [N.m.s.rad ⁻¹]	0.08
Number of pole pairs, p	2

DC-Side Controller	
Proportional gain of DC voltage controller, K_{pdc}	2
Integral gain of DC voltage controller, K_{idc}	100

Source-Side Controller	
Proportional gain of current controller, K_{pc}	6
Integral gain of current controller, K_{ic}	4500

Battery	
Battery type	Li-Ion
Nominal Voltage (V)	200
Rated Capacity (Ah)	6.5
Battery response time (s)	3600

DC/DC Buck-Boost converter	
Battery resistance, R_b [Ω]	5
Battery inductance, L_b [mH]	20
Switching frequency, f_{sw} [kHz]	25

Battery-Side Controller	
Proportional gain of voltage controller, K_{pvB}	1
Integral gain of voltage controller, K_{ivB}	25
Proportional gain of current controller, K_{piB}	6
Integral gain of current controller, K_{iiB}	900

Table 2: Parameters of the PI controllers of the IFOC blocks.

IFOC	
Proportional gain of speed controller, K_{ps}	30
Integral gain of speed controller, K_{is}	200

APPENDIX B

B.1 Modelling and MPPT strategy for wind turbine

The relationship between the aerodynamic power extracted from the wind and the wind speed is given as follows [45-51]:

$$P_m = \frac{1}{2} \pi \rho C_p(\lambda, \beta) R^2 v^3 \quad (5)$$

Where P_m is the mechanical power of the wind turbine and β [degrees] represents the pitch angle of the blades. The power coefficient C_p defines the aerodynamic efficiency of the wind turbine. One of the basic equations used to model C_p , which is a function of the speed ratio λ and the pitch angle β of the blade, can be expressed as follows:

$$C_p(\lambda, \beta) = 0.5 \left[\frac{33}{\lambda_i} - 0.2\beta - 0.4 \right] e^{-\frac{12.7}{\lambda_i}} \quad (6)$$

$$\frac{1}{\lambda_i} = \frac{1}{\lambda + 0.08\beta} - \frac{0.035}{\beta^3 + 1} \quad (7)$$

$$\lambda = \frac{\Omega_m R}{v} \quad (8)$$

Where Ω_m [rad/s] denotes the mechanical speed of the turbine.

The MPPT methodology is derived from the following relation:

$$P_{m,max} = K_{p,opt} \cdot \Omega_{m,opt}^3 \quad (9)$$

Where $\Omega_{m,opt}$ is the mechanical speed at which the turbine extracts the maximum power from the wind and is denoted as $P_{m,max}$. The controller gain $K_{p,opt}$ is derived as:

$$K_{p,opt} = \frac{1}{2} \rho C_{p,max} \frac{R^5}{\lambda_{opt}^3} \quad (10)$$

Where ρ is the density area [kg.m⁻²], $C_{p,max}$ is the maximum power coefficient and λ_{opt} represents the optimal tip speed ratio. The corresponding optimal mechanical torque is:

$$T_{m,max} = \frac{P_{m,max}}{\Omega_{m,opt}^3} \quad (11)$$

Fig. 23 shows the maximum power characteristics of the turbine obtained from equations (5 and 9).

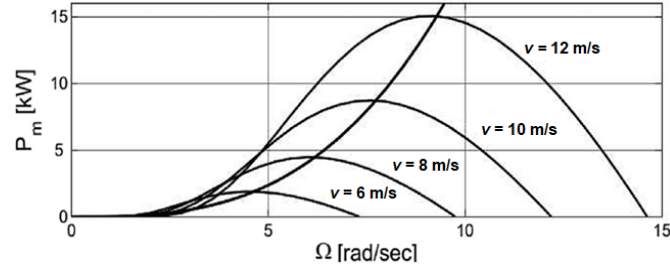


Fig. 23 Optimum operating characteristics of the wind turbine.

B.2 Strategy the control of the generator side

Let the flux ϕ_r be oriented on the d-axis and considering the equations of the fluxes and voltages, the control variables v_{sd} and v_{sq} are obtained as follows:

$$\begin{cases} v_{sd} = \left[R_s + L_s \sigma \frac{d}{dt} \right] i_{sd} - \omega_s L_s \sigma i_{sq} \\ v_{sq} = \left[R_s + L_s \sigma \frac{d}{dt} \right] i_{sq} + \omega_s L_s \sigma i_{sd} + \frac{L_m}{L_r} \omega_s \phi_r \\ T_r \frac{d\phi_r}{dt} + \phi_r = L_m i_{sd} \\ \frac{L_m}{T_r} i_{sq} = \omega_{slip} \phi_r \\ T_{em} = p \frac{2}{3} \left[\frac{L_m}{L_r} \right] \phi_r i_{sq} \end{cases} \quad (12)$$

In steady-state, the above equations can be written as:

$$\begin{cases} v_{sd} = R_s i_{sd} - \omega_s L_s \sigma i_{sq} \\ v_{sq} = \omega_s L_s i_{sd} + R_s i_{sq} \end{cases} \quad (13)$$

Similarly, the steady-state equation of the flux becomes:

$$\phi_r = L_m i_{sd} \Rightarrow i_{sd} = \frac{\phi_r}{L_m} \quad (14)$$

When the machine operates at the base speed, the stator flux is equal to its nominal value ϕ_{sn} . For speeds above the base speed, since the voltage cannot be increased further, the flux must be reduced. This is known as field weakening and is defined as follows:

$$\phi_{sref} = \begin{cases} \phi_n & \text{if } |\Omega_r| \leq \Omega_n \\ \frac{\Omega_n}{|\Omega_r|} \phi_n & \text{if } |\Omega_r| \geq \Omega_n \end{cases} \quad (15)$$